

Numerical Investigation of Laser Oscillation in a Recombining Hydrogen Plasma Interacting with Helium Gas in TPD-I

Toshiatsu Oda

Department of Applied Physics and Chemistry, Faculty of Engineering,
Hiroshima University, Saijo, Higashihiroshima 724, Japan

Utarō Furukane

Department of Physics, College of General Education, Ehime University, Matsuyama 790, Japan

Z. Naturforsch. **40a**, 485–489 (1985); received January 29, 1985

A numerical investigation on the basis of a collisional-radiative (CR) model has shown that laser oscillation between the levels with the principal quantum numbers $i = 2$ and 3 can be generated in a recombining hydrogen plasma interacting with a dense helium gas as a cooling medium in TPD-I, which is a magnetically confined quiescent high-density plasma source consisting basically of two parts, namely, the discharge region with the cathode at the center of the cusped magnetic field and the plasma column region with the axial magnetic field. The population inversion is found to exceed significantly a threshold level for the laser oscillation even in the quasi-steady state when the hydrogen plasma with $n_e = 10^{13} \sim 10^{14} \text{ cm}^{-3}$ interacts with the helium gas with a pressure of about 50 Torr.

1. Introduction

The high potentiality of shortwave-laser action in recombining plasmas has been widely recognized. In general, there are three different experimental approaches to produce the recombining plasmas: (i) a short-pulsed high power laser beam is injected into a gas to produce a hot plasma, which is then cooled by radiation loss [1], (ii) a dense and hot plasma produced by arc discharge [2] is freely expanded in a vacuum vessel, (iii) a stationary plasma is made to interact with a cool and dense neutral gas [3]. The third one is superior to the two others in the following two points: A stationary population inversion is produced, and the plasma parameters are easily controlled.

In a previous paper [4] we have investigated the processes leading to the population inversion between the levels with the principal quantum numbers 3 and 4 in a recombining hydrogen plasma which is interacting with a cool and dense neutral hydrogen gas by using the rate equations on the basis of a collisional-radiative (CR) model and the energy equations for electrons, ions and neutral particles.

In this case, the population inversion between the levels 2 and 3 , which is more important for the

generation of a short-wave laser, however, is hardly to be expected because the plasma is optically thick against the L_α line and the population density of the level 2 , n_2 , is not sufficiently decreased owing to the increase of the population density of the ground level during the contact of the hydrogen gas with the plasma. In order to realize laser action between the levels 2 and 3 we can simply use an other neutral gas, for example helium instead of hydrogen to cool the high temperature hydrogen plasma as pointed out in [4].

In the present paper, we investigate laser oscillation between the levels 2 and 3 in a recombining hydrogen plasma which is interacting with a dense helium gas by using the same method as that in [4].

2. Description of the Calculation

We consider the elastic collisional processes between electrons and atoms, electrons and ions, and atoms and ions. The following inelastic collisional and radiative processes considered here:

$$(A) \quad a_i + e \rightleftharpoons a_k + e, \quad (k > i),$$

$$(B) \quad a_i + e \rightleftharpoons a_+ + e + e,$$

$$(C) \quad a_+ + e \rightarrow a_i + h\nu,$$

$$(D) \quad a_k \rightarrow a_i + h\nu, \quad (k > i),$$

where a_i denotes an excited hydrogen or helium atom in level i , a_+ an ionized hydrogen or helium

Reprint requests to Dr. T. Oda, Faculty of Engineering,
Hiroshima University, Higashihiroshima 724, Japan.

0340-4811 / 85 / 0500-0485 \$ 01.30/0. – Please order a reprint rather than making your own copy.



Dieses Werk wurde im Jahr 2013 vom Verlag Zeitschrift für Naturforschung in Zusammenarbeit mit der Max-Planck-Gesellschaft zur Förderung der Wissenschaften e.V. digitalisiert und unter folgender Lizenz veröffentlicht: Creative Commons Namensnennung-Keine Bearbeitung 3.0 Deutschland Lizenz.

Zum 01.01.2015 ist eine Anpassung der Lizenzbedingungen (Entfall der Creative Commons Lizenzbedingung „Keine Bearbeitung“) beabsichtigt, um eine Nachnutzung auch im Rahmen zukünftiger wissenschaftlicher Nutzungsformen zu ermöglichen.

This work has been digitalized and published in 2013 by Verlag Zeitschrift für Naturforschung in cooperation with the Max Planck Society for the Advancement of Science under a Creative Commons Attribution-NoDerivs 3.0 Germany License.

On 01.01.2015 it is planned to change the License Conditions (the removal of the Creative Commons License condition “no derivative works”). This is to allow reuse in the area of future scientific usage.

atom, e an electron, and $h\nu$ a photon. We use the same coordinate as that in [4], where the plasma flows with a constant speed of v_0 . The rate equation for the population density n_i of hydrogen ($1 \leq i \leq 20$) is given by

$$\frac{dn_i}{dt} = \sum_{j=1}^{20} a_{ij} n_j + \delta_i, \quad 1 \leq i \leq 20. \quad (1)$$

Here a_{ij} and δ_i are given in terms of the rate coefficients for the radiative and electron-collision processes as in [4], and the maximum quantum number is chosen to be 20 as was done by Cacciatore and Capitelli [5]. A rate equation very similar to (1) is used for the population density n_i^{He} of helium. The He(I) levels are treated in much the same way as by Drawin [6]. We consider all the sublevels as individual levels having different orbital angular momenta l for the principal quantum numbers $n \leq 2$. For the levels $3 \leq n \leq 19$, all the sublevels are grouped together. The total number of levels involved in the rate equations for He(I) is thus 39. The rate coefficients are used as in [6]. For simplicity, the inelastic atom-atom collisions are neglected. The term for the particle flux in radial direction is neglected in the neighborhood of the center axis of the plasma column.

The electron density n_e is given by

$$\frac{dn_e}{dt} = - \sum_{j=1}^{20} \frac{dn_j}{dt} - \sum_{j=1}^{20} \frac{dn_j^{\text{He}}}{dt}. \quad (2)$$

The energy equation used for the electrons is very similar to that in [4], except that the corresponding elastic and inelastic collision terms for helium are included in the present case. We have

$$\begin{aligned} \frac{dT_e}{dt} = & \frac{1}{\tau_{eH}} (T_H - T_e) + \frac{1}{\tau_{eH^+}} (T_{H^+} - T_e) \\ & + \frac{1}{\tau_{eHe}} (T_{He} - T_e) + \frac{1}{\tau_{eHe^+}} (T_{He^+} - T_e) \\ & + \left[- \sum_{\substack{j < k \\ k=2}}^{20} (E_j - E_k) (C_{jk} n_j - F_{kj} n_k) \right. \\ & \left. - \sum_{j=1}^{20} (E_j + \frac{3}{2} T_e) K_{jc} n_j \right. \\ & \left. + n_e n_+ \sum_{j=1}^{20} (E_j + \frac{3}{2} T_e) K_{cj} \right]_{\text{H}} + \frac{2}{3} [\dots]_{\text{He}} \end{aligned} \quad (3)$$

where $[\dots]_{\text{He}}$ is the term for helium corresponding to the fifth one for hydrogen on the r.h.s. The electron-atom and electron-ion collision times of hydrogen (τ_{eH} and τ_{eH^+}) are given in [4], and the corresponding collision times of helium (τ_{eHe} and τ_{eHe^+}) in [7] and [8]. We also neglect the term for the spatial divergence in the radial direction in (2) and (3) as in (1).

All the optical escape factors are set equal to one, that is, the plasma is considered to be optically thin because the interacting gas is not hydrogen but helium.

The initial conditions for the numerical calculations are the following: the hydrogen plasma is in a stationary state (the electron, ion and atom temperatures being expressed as T_{e0} , T_{i0} and T_{H0} , respectively, and the electron density as n_e), and is brought into interaction with neutral helium gas of high density n_0^{He} at $t = 0$, all the helium atoms being in the ground state at an initial atom-temperature of T_{a0} . For simplicity, we assume that $T_i = T_H = T_{He}$ are all kept constant throughout the reactions considered here. We have made the calculations for the three initial temperature and density conditions shown in Table 1. In case 1, n_{e0} is low, while it is high in case 2. The case 3 represents an extreme plasma whose electron density exceeds the upper bound value for the population inversion in the quasi-stationary state QSS [9]. This case is chosen in order to show whether the population inversion takes place in the transient phase of the recombining plasma whose electron density is so high that the population inversion cannot be expected in the QSS.

The QSS assumption is made for the levels higher than a certain one as discussed in [4]. We made time integration of the equations by using the same calculating procedure as described in [4].

Table 1. Initial conditions and the relaxed electron temperature T_{er} .

	T_{e0} (eV)	T_{i0} (eV)	n_{e0} (cm ⁻³)	n_0 (cm ⁻³)	n_0^{He} (cm ⁻³)	T_{er} (eV)
1	5	0.05	6.3×10^{13}	5.1×10^9	2×10^{18}	0.078
2	5	0.05	2.0×10^{14}	1.6×10^{10}	2×10^{18}	0.43
3	5	0.05	1.0×10^{15}	1.3×10^{11}	1×10^{20}	0.45

3. Results and Discussion

Let us first describe the temporal behavior of T_e , which is the most important one for realizing population inversion.

Figure 1 shows a rapid decrease of T_e after the neutral gas is introduced. In the case 1, T_e decreases to as low a value as 0.074 eV, while T_e in the cases 2 and 3 decreases to only 0.43 eV. This is because n_e is in the cases 2 and 3 much higher than in case 1.

On the other hand, the decrease of T_e in the case 3 begins earliest of all three cases. Times of establishment of QSS in each case are shown by the arrows labeled $t_Q(1)$, etc. The plasma in case 3 reaches the QSS earliest because the helium atom density is 50 times higher than in the other cases.

The population density n_i ($i = 1, 2, 3$) of atomic hydrogen divided by the statistical weight ω_i , versus time in the case 1 is shown in Figure 2. As is expected, n_1 keeps almost constant until just prior to the beginning of the QSS, and increases up to beyond 10^{12} cm^{-3} after $t = 1 \mu\text{s}$. In this phase ($n_1 > 10^{12} \text{ cm}^{-3}$), our assumption of an optically thin plasma may not be valid when the plasma has the mean radius $r_0 > 0.84 \text{ cm}$ [10]. It should be noted that population inversion takes place as early as at

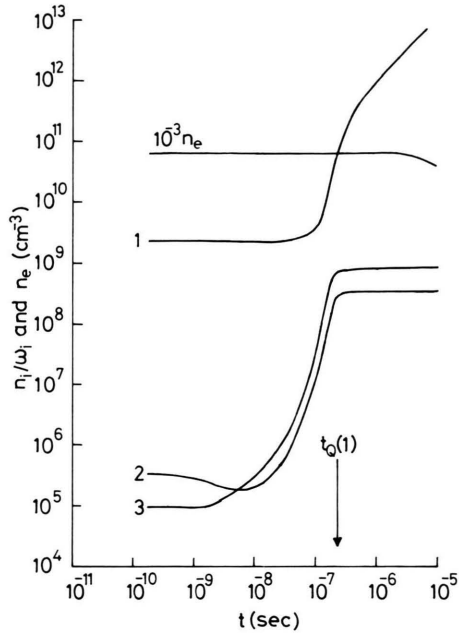


Fig. 2. Temporal behavior of the population densities n_i ($i = 1, 2, 3$) and the electron density n_e in the case 1.

$t = 6 \times 10^{-9} \text{ s}$. Then both n_2 and n_3 increase with time till $t = 3 \times 10^{-7} \text{ s}$ when the QSS is realized. The population inversion itself becomes maximum in the QSS. A similar behavior in n_i/ω_i is obtained in the case 2 (Figure 3). But the population inversion becomes smaller.

The evolution of n_i/ω_i in the case 3 is shown in Figure 4. In this case, the inversion starts as early as at 10^{-9} s and becomes the largest of the three cases. But the inversion disappears a little bit before the QSS is established at $t = 10^{-8} \text{ s}$ since n_e exceeds the upper bound value for the generation of population inversion [9] as described before.

In order to compare in more detail the above described three kinds of the results, we demonstrate the evolution of the overpopulation density $\Delta n_{32} (= n_3/\omega_3 - n_2/\omega_2)$ in Fig. 5, which is obtained from the results shown in Figures 2–4. In the regions of $\Delta n_{32} < 0$, that is no population inversion, no curves are indicated. The horizontal broken line shows a threshold value of Δn_{32} for the laser oscillation under the condition that the optical cavity consists of two plane mirrors with reflectivity of 99% for one and 99.8% for the other and that the plasma column has a length of 10 cm [11].

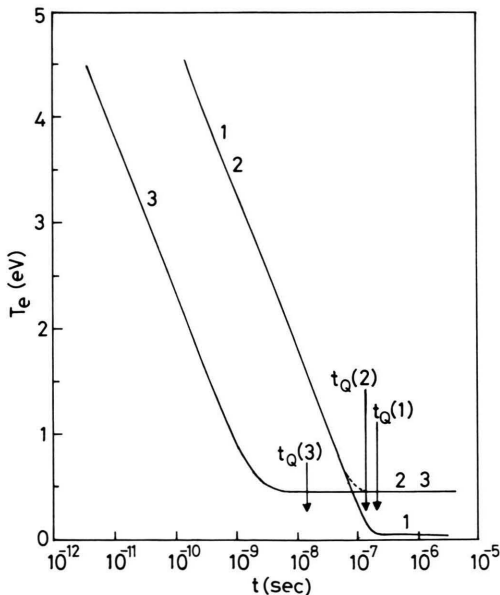


Fig. 1. Electron temperature vs. time period. $T(1)$ means the temperature in the case 1, etc. The arrows labeled $t_Q(1)$ show the time of establishment of the QSS in the case 1, and so on.

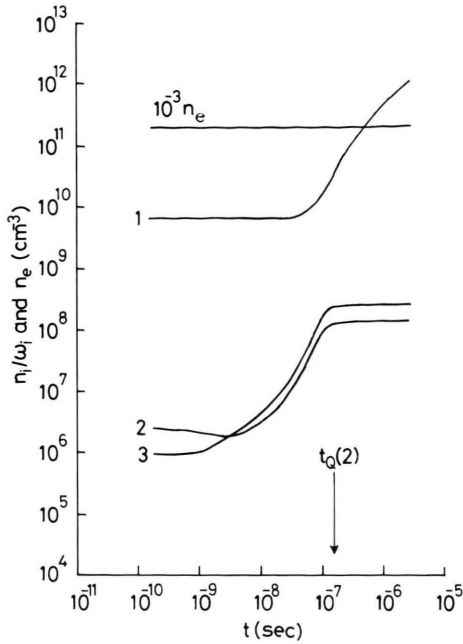


Fig. 3. Temporal behavior of the population densities n_i ($i = 1, 2, 3$) and the electron density n_e in the case 2.

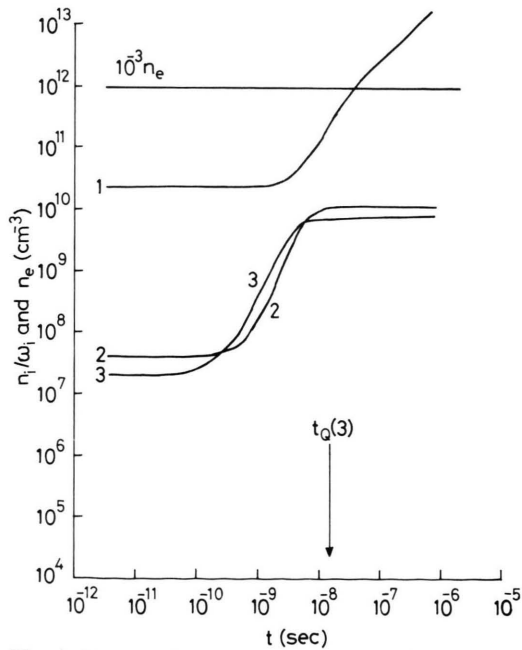


Fig. 4. Temporal behavior of the population densities n_i ($i = 1, 2, 3$) and the electron density n_e in the case 3.

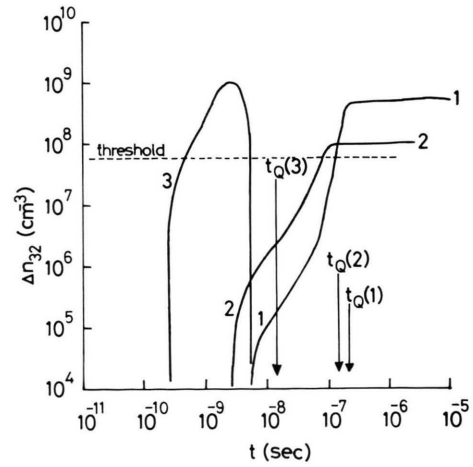


Fig. 5. The evolution of overpopulation density Δn_{32} in the cases 1, 2, and 3. In the regions where no curves appear, Δn_{32} is negative, that is, there is no population inversion.

Δn_{32} is higher in the case 2 than in the case 1 in the transient phase before the QSS is achieved. The reason is that the recombination process is more dominant in the case 2 because of the high electron density. On the contrary, Δn_{32} is higher in the QSS because T_{er} is lower in the case 1 than in the case 2. The laser action thus will be easier in the case 1.

In the case 3, the population inversion takes place as early as at $t = 3 \times 10^{-10}$ s, which is earliest in the three case, because T_e is decreased rapidly. It should be noted that Δn_{32} exceeds largely the threshold level for the laser oscillation. In the QSS, however, the inversion disappears owing to the above described reason.

It should be noted that the laser oscillation is expected in all three cases when helium is used instead of hydrogen in order to cool the hydrogen plasma.

4. Conclusion

Our calculations have shown that population inversion between the levels 2 and 3 of the hydrogen atom can be generated in a recombining hydrogen plasma which is interacting with helium. This plasma is superior to the plasma described in [4] in that the population density of the ground state does almost not increase in the transient recombining phase because helium is introduced instead of hydrogen.

It is important that Δn_{32} is higher than the threshold level for the laser oscillation even in the QSS when the hydrogen plasma with $n_e = 10^{13} \sim 10^{14} \text{ cm}^{-3}$ interacts with the helium at a pressure of ~ 50 Torr.

In conclusion, laser oscillation is certainly expected in all these three cases.

Acknowledgements

This work was carried out as part of collaboration at the Institute of Plasma Physics, Nagoya University. The numerical calculations have been made at the Computer Center of the Institute of Plasma Physics, Nagoya University and at the Computer Center in Ehime University.

- [1] S. Suckewer, C. H. Skinner, D. R. Voorhees, H. M. Milchberg, C. Keane, and A. Semet, *IEEE J. Quantum Electron.* **QE-19**, 1855 (1983).
- [2] T. Hara, K. Kodaera, M. Hamagaki, K. Matsunaga, M. Inutake, and T. Dote, *Japan. J. Appl. Phys.* **19**, L606 (1980).
- [3] K. Sato, M. Shiho, M. Hosokawa, H. Sugawara, T. Oda, and T. Sasaki, *Phys. Rev. Lett.* **39**, 1074 (1977).
- [4] U. Furukane and T. Oda, *Z. Naturforsch.* **39a**, 132 (1984).
- [5] M. Cacciatore and M. Capitelli, *Z. Naturforsch.* **29a**, 1507 (1974).
- [6] H. W. Drawin and F. Emard, Fontenay-aux-Roses Report No. EUR-CEA-FC-534, 1970 (unpublished).
- [7] D. Barbere, *Phys. Rev.* **84**, 653 (1951).
- [8] L. Spitzer, Jr., *Physics of Fully Ionized Gases*, 2nd Ed., John Wiley, New York 1961, p. 135.
- [9] U. Furukane, T. Yokota, and T. Oda, *J. Quant. Spectr. Radiat. Transfer* **22**, 239 (1979).
- [10] U. Furukane, T. Yokota, K. Kawasaki, and T. Oda, *J. Quant. Spectral. Radiat. Transfer* **29**, 75 (1983).
- [11] T. Oda and U. Furukane, *J. Quant. Spectr. Radiat. Transfer* **29**, 553 (1983).